Geomechanics and Engineering, *Vol. 18, No. 3 (2019) 259-266*
DOI: https://doi.org/10.12989/gae.2019.18.3.259

Experimental observation and numerical simulation of cement grout penetration in discrete joints

Jong-Won Lee[1,3a], Hyung-Mok Kim[*1], Mahmoud Yazdani[2b], Hangbok Lee[3c], Tae-Min Oh[4d] and Eui-Seob Park[3e]

[1]*Department of Energy & Mineral Resources Engineering, Sejong University, Seoul 05006 Korea*
[2]*Department of Civil and Environmental Engineering, Tarbiat Modares University, Tehran 14117-13116 Iran*
[3]*Center for Deep Subsurface Research, Korea Institute of Geoscience and Mineral Resources (KIGAM), Daejeon 34132 Korea*
[4]*Department of Civil and Environmetnal Engineering, Pusan National University, Busan 46241 Korea*

(Received May 28, 2018, Revised April 28, 2019, Accepted June 3, 2019)

Abstract. This paper presents a comparison between experimental measurements and numerical estimations of penetration length of a cement grout injected in discrete joints. In the experiment, a joint was generated by planar acryl plates with a certain separation distance (; aperture) and was designed in such a way to vary the separation distances. Since a cement grout was used, the grout viscosity can be varied by controlling water-cement (W/C) ratios. Throughout these experiments, the influence of joint aperture, cement grout viscosity, and injection rate on a penetration length in a discrete joint was investigated. During the experiments, we also measured the time-dependent variation of grout viscosity due to a hardening process. The time-dependent viscosity was included in our numerical simulations as a function of elapsed time to demonstrate its impact on the estimation of penetration length. In the numerical simulations, Bingham fluid model that has been known to be applicable to a viscous cement material, was employed. We showed that the estimations by the current numerical approach were well comparable to the experimental measurements only in limited conditions of lower injection rates and smaller joint apertures. The difference between two approaches resulted from the facts that material separation (; bleeding) of cement grout, which was noticeable in higher injection rate and there could be a significant surface friction between the grout and joint planes, which are not included in the numerical simulations. Our numerical simulation, meanwhile, could well demonstrate that penetration length can be significantly over-estimated without considering a time-dependency of viscosity in a cement grout.

Keywords: cement grout; penetration length; Bingham fluid; time-dependent viscosity

1. Introduction

Injection of cement grout is very popular in variety fields of civil and geotechnical engineering, which are represented by a dam foundation (Jones *et al.* 2018) and an underground construction work (Jamsawang *et al.* 2017). Clay and chemical grouts are normally too expensive and cement give a more economical and durable in underground constructions (Houlsby 1990).

The primary objective of grouting in underground construction of rock is typically either to control water inflow, to strengthen a surrounding ground or both. All rock grouting, thus, involves the filling of existing fractures and joints and this is usually accomplished with cementitious grouts (Warner 2004).

Underground construction, particularly in deep depths, is usually involved with a jointed rock mass. Injected grout in a subsurface jointed rock mass flows mainly through connected individual joints. Hence, the grout flow behavior should be first clearly understood in a single rock joint to be able to study grouting behavior in the jointed rock masses which containing multiple individual joints to be connected with each other. Although, the theory of grouting in rock joints is well established and the grouting performance can be estimated on a basis of good characterization of jointed rock mass, it is still difficult to accomplish a grouting exactly as designed and obtain the grouting performance as estimated, compared to homogeneous soil grouting (Zheng *et al.* 2016).

Grout penetration in a discrete joint has been extensively investigated either experimentally or numerically and reported that penetration is subject to mainly grout material properties and geometry of joint (Azimian and Ajalloeian 2015, Funehag and Thörn 2018, Chegbeleh *et al.* 2009, Hassler *et al.* 1991, Ghafar *et al.* 2017, Minto *et al.* 2016, Mohammed *et al.* 2015, Rahman *et al.* 2017, Saedi *et al.* 2013, Sohrabi-Bidar *et al.* 2016, Sui *et*

*Corresponding author, Professor
E-mail: hmkim@sejong.ac.kr
[a]Researcher
E-mail: leejongwon@kigam.re.kr
[b]Assistant Professor
E-mail: myazdani@modares.ac.ir
[c]Senior Researcher
E-mail: leehb@kigam.re.kr
[d]Assistant Professor
E-mail: geotaemin@pusan.ac.kr
[e]Principle Researcher
E-mail: espark@kigam.re.kr

http://www.techno-press.org/?journal=gae&subpage=7
ISSN: 2005-307X (Print), 2092-6219 (Online)

al. 2015, Tani 2012, Xiao *et al.* 2017). The comparison, however, between both experiments and numerical simulations have been seldom published.

Viscosity of cement grout is one of the influential parameters governing the penetration length which can even vary during the period of injection due to its hardening process. Kobayashi and Stille (2007) has first reported that the viscosity increment along with its hardening may reduce the penetration length remarkably depending on the level of water to cement (*W/C*) ratio. A time-dependent model of the cement viscosity thus should be established in a proper manner through laboratory experiments to be used in estimating grout injection performance by numerical approach.

Applicability of Bingham fluid model and its theoretical development in simulating a cement grout flow was first contributed by Gustafson and Stille (2005) and followed by Tani and Stille (2017) and Gustafson *et al.* (2013). Using coupled hydraulic-mechanical simulation of 1D Bingham flow through a single joint, authors have demonstrated that joint aperture change, induced by injection pressure, may affect the grout penetration length significantly (Kim *et al.* 2018). In the simulations, the effect of injection-induced aperture change were studied on penetration length and they were in a good agreement with the available analytical solution (Gustafson and Stille 1996). We extended our numerical simulation to 2D in this study but, only the hydraulic analysis was used, since the grout injection pressure was not sufficient enough to cause a mechanical deformation of joint aperture.

In this paper, cement grout penetration behavior in a circular planar joint is investigated both experimentally and numerically. The numerical results of the grout penetration is verified by means of experimental observation of penetration behavior in a smooth wall joint. The Bingham fluid model in UDEC, which should be adequate within the range of *W/C* ratio between 1.0 and 2.0 (Li *et al.* 2017), is adopted to simulate a viscous cement grout flow in the joint.

2. Experimental measurements of viscosity and penetration length of cement grout

2.1 Time-dependent viscosity of cement grout

Viscosity of cement grout can be subject to elapsed time after its mixing and injection. The viscosity usually increases in proportional to the elapsed time due to a hardening process of cement and affects a flow behavior in rock joints (Kobayashi and Stille 2007).

Before injection, we measured a time-dependency of viscosity of cement grout, which was used in the experiments of penetration length measurements, and expressed it as a function of elapsed time to implement it in our subsequent numerical simulation, which should be more usefully effective than experimental approach in investigating its influence on penetration length. For the measurement, we used a specialized viscometer. Viscosity is a measure of fluid's resistance to flow so that the principal of measuring viscosity by the viscometer is to drive a

Table 1 The physical properties of the micro cement used in the experiment

Properties	Unit	Value
Fineness	cm^2/g	Over 8,000
Setting time	minutes	Over 60
Compressive strength (3/7/28 days)	MPa	20/40/50
Average particle size	μm	5±1
Chemical composition (SO_3/ lg.Loss)	%	Under 5.0/3.0

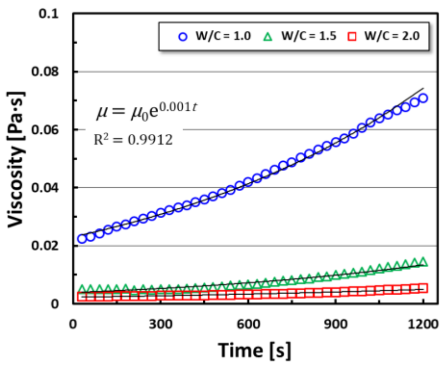

Fig. 1 The viscosity measurements of cement grout as a function of elapsed time (dots: the experimental measurements, lines: the fitted exponential function)

spindle, which is immersed in a cement grout reservoir, through a calibrated spring and to obtain a viscous drag of the cement grout against the spindle by the spring deflection. The measurement of this kind is quite popular since Hakansson *et al.* (1992), and the measurement range of the viscometer is determined by the rotational speed of the spindle, the size and shape of the spindle, the container the spindle is rotating in, and the torque of the calibrated spring. The rotary viscometer with cylindrical spindle (ULA adaptor which can measure with shear rate range of 0.6~244.6 s^{-1}) used in this study can measure a viscosity within the range of 100 to 40 million centipoise (cP, equal to 10^{-3} Pa s) which fully covers typical values of cement and microfine cement grouts from several hundreds to thousands cP (Struble and Sun, 1995).

Physical properties of cement grout used in the study are the same as our previous experimental work (Lee, 2017). It was a micro-cement of MICEM 8000 and the details of the cement is presented in Table 1, in which typical grain size distribution of D_{95} is less than 16 μm and a specific gravity is 2.95. The cement grout was prepared by mixing with a hand-mixer for 1 minute at 20°C of room temperature. To verify the flow characteristics of grout without unintended effect, an additive was not considered in this study.

Fig. 1 shows the viscosity measurements of cement grout with two representative water-cement (*W/C*) ratios of 1.0 and 2.0 at various elapsed times. The measurements are shown as dots in the figure and the lines are the best fitted functions to the measurements. The viscosity, similar to Kobayashi and Stille (2007), increased in proportional to elapsed time and its time-dependent evolution was to be represented as an exponential function of time. It was also noted that the time-dependent increment was more remarkable in the relatively lower *W/C* ratio, for example, the viscosity of *W/C* ratio of 1.0 was about 14 times of that in *W/C* ratio of 2.0 at the elapsed time of 1,200 seconds, which may result in a considerable difference in the estimation of penetration length. The effect of time-dependent variation of grout viscosity was further investigated in detail using the obtained function by numerical simulations.

2.2 Penetration of cement grout in a discrete joint

It is a penetration length that is usually measured to evaluate the performance of cement grout injection into a discrete joint. In this study, a particular experimental set-up was designed to measure a penetration length of grout. The cement grout was injected into the planar joint that was generated by an acryl plates and was representing a discrete fracture or joint.

Fig. 2 shows the experimental apparatus used in measuring a penetration length, which consists of a syringe pump and a control system to regulate injection rate provided from a reservoir tank of cement grout, a transparent acryl planar specimen embedding a single joint with a separation distance i.e. aperture, and a digital camera to take a picture of the penetration length at a certain elapsed time after injection. The acryl planar specimen consisted upper and lower plate with acrylic ring to control and maintain the aperture size of 1, 3, and 5 mm. In addition, the test specimen was bolted along the outside line of specimen. Since injection is conducted at the center of the planar joint, the grout penetrates in a radial form, which is quite often in a fluid flow in rock fractures (NRC, 1996). The grout penetration length, thus, corresponds to the radius of circular penetration region of injected grout. In the experimental measurements, however, the penetration region did not necessarily follow an ideal circular shape, and thus an average radius was referred to a penetration length.

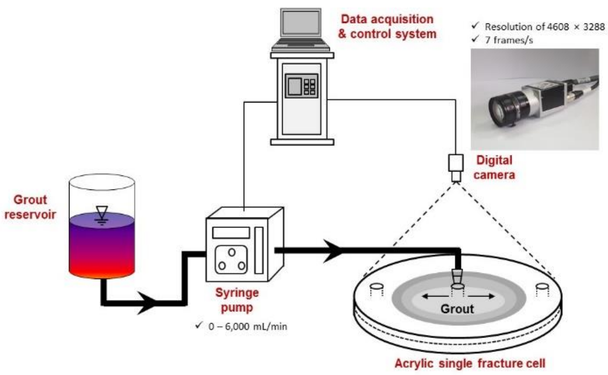

(a) Schematic diagram of the experimental set-up

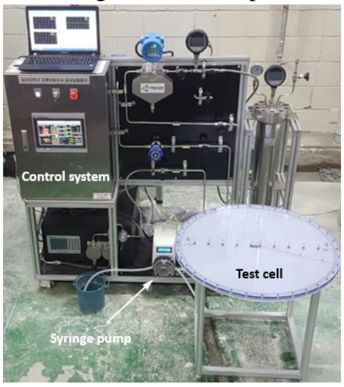

(b) Photo of the experimental set-up

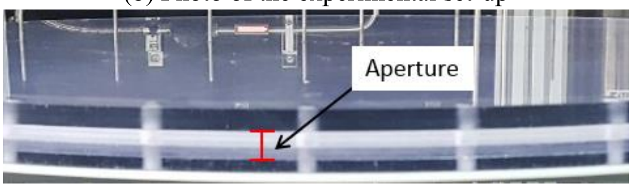

(c) Side view of the circular planar joint

Fig. 2 Experimental set-up for the injection test of cement grout in the circular planar joint (Lee 2017)

Rock joints can be either unsaturated or saturated with fluid, mainly water in most cases. There is not fluid present but filled with air of atmospheric pressure in the joint of our experiment and is corresponding to completely unsaturated condition.

The reference conditions of our grout injection experiments are injection rate of 200 ml/min, aperture of 1 mm, and water/cement ratio of 1.0 and the effect of each parameters was investigated by changing them to different values when other parameters are kept constant.

2.2.1 The effect of injection rate on penetration length

The effect of injection rate was examined by measuring and comparing penetration lengths at three different injection rates of 200, 400, and 600 ml/min. Injection rate is closely related to pressure dissipation within a joint and the range of injection rates in the test were determined such that the dissipation pressure and penetration length of injected cement grout could be controlled in a stable manner under the present experimental set-up.

Fig. 3 shows that the grout penetration lengths are increasing in proportion to the injection rates. In the previous analytical solution of Gustafson & Stille (1996), penetration length is a function of square root of injection rate so that the penetration lengths of injection rate of 400 ml/min and 600 ml/min should be equal to the 1.4 ($\approx \sqrt{(400/200)}$) and 1.7 ($\approx \sqrt{(600/200)}$) times of that in the reference case, in which the injection rate was 200 ml/min. In the experiment, we could observe similar results that the penetration lengths at 20 seconds of 400 ml/min and 600 ml/min were 15.2 cm and 18.5 cm, which correspond to the 1.42 and 1.72 times of that in the reference case of 10.7 cm for 200 ml/min. The relation between the penetration length and injection rate, however, deviated from the square root relationship at a later stage of injection, especially in the conditions of relatively larger injection rate. The reason of the deviation can be explained by material separation (; bleeding) and air bubbles, that are often formed in cement grout mixing and injection (Warner 2004), which was distinctly observed in our previous experiments and became more distinct in our subsequent numerical simulation as well (Lee *et al.* 2017).

2.2.2 The effect of joint aperture on penetration length

A series of grout injection tests was conducted on planar

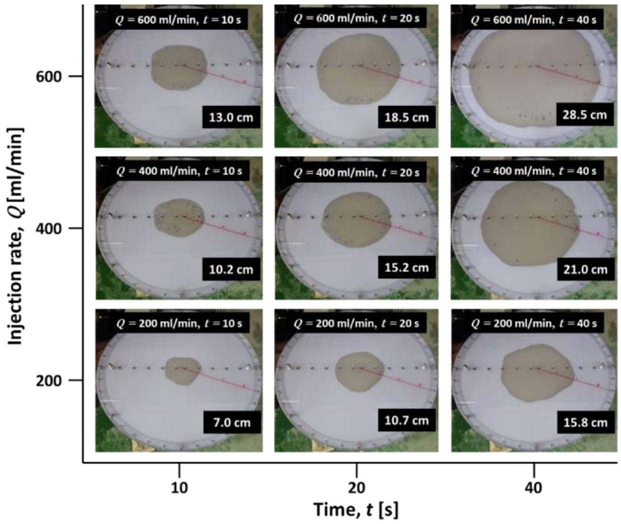

Fig. 3 The measured grout penetration lengths under different injection rates (Q : injection rate, t : elapsed time)

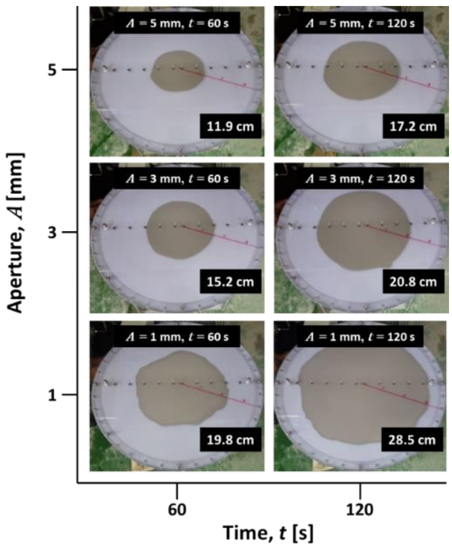

Fig. 4 The measured grout penetration lengths under different joint apertures (A: joint aperture, t : elapsed time)

specimen with three different apertures of 1mm, 3mm and 5 mm, which are the typical values of in-situ rock fractures (NRC, 1996). Fig. 4 shows the observed penetration length at each aperture condition. Note that the cement grout in this study is injected at constant volumetric rate, which is quite common in practice, such that the penetration length is relatively larger in smaller aperture conditions. At a constant pressure condition, on the contrary, the penetration length may increase along with aperture increment.

As was different from the analytical solution by Gustafson and Stille (1996), in which aperture increment resulted in linear proportional relationship with penetration length, distinct proportionality could not be observed in the experiment. This, especially in the case of the smaller aperture condition, could be attributed to a surface friction in the interface between the joint and injected grout,

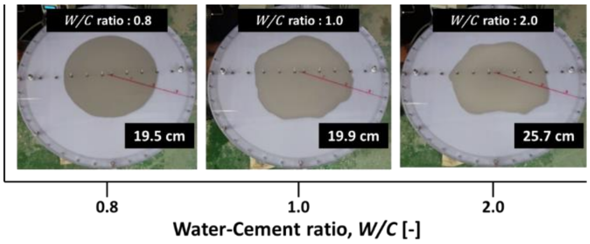

Fig. 5 The measured grout penetration lengths under different W/C ratios (The penetration length value at each case was shown in the figure)

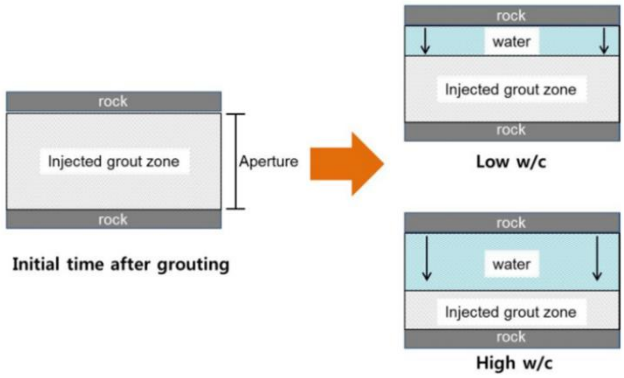

Fig. 6 Schematic diagram of the bleeding behavior of the cement grout with higher W/C ratio (Lee *et al.* 2017)

although the joint surface was comparatively by far smoother than in-situ rock joint surfaces.

2.2.3 The effect of W/C ratio on penetration length

Fig. 5 shows the cement grout penetration behaviour at different W/C ratio conditions. It is noted that the grout penetrated region deviates from an ideal circular shape when W/C ratio of cement grout becomes larger possibly due to its lower viscosity with higher water content in the grout. In the case of higher water content as well as relatively large aperture conditions, bleeding to the direction of gravity was distinctly observed (Fig. 6), which resulted in the increment of penetration length.

3. Numerical simulation of cement grout penetration in a planar joint

Numerical analysis of cement grout penetration in a planar joint is carried out using viscous fluid flow model in UDEC (Itasca 2014). As it is common in the grouting industry, the cement grout is assumed to follow the Bingham fluid flow model, characterized by a yielding shear strength (τ_0) over which the fluid starts to flow.

The Bingham fluid model in UDEC computes the flow rate (q) using Buckingham's equation (Wilkinson 1960) as

$$q = \frac{\pi r^4}{8\mu_g}\frac{\Delta p}{L}\left[1 - \frac{4}{3}\left(\frac{2\tau_0}{r}\frac{L}{\Delta p}\right) + \frac{1}{3}\left(\frac{2\tau_0}{\Delta p}\right)^4\right] \quad (1)$$

where, r is the radius of fictitious circular pipe, μ_g is the viscosity, Δp is the pressure gradient, and L is the flowing length.

Table 2 Material properties used in the numerical simulation as a reference case

Intact rock block properties:			
Density [kg/m^3]	Bulk modulus [GPa]		Shear modulus [GPa]
3,000	10		3
Fluid properties:			
Density [kg/m^3]	Bulk modulus [GPa]	Viscosity [Pa·s]	Yield strength [Pa]
1.48	2	0.0135	0.3067
Joint properties			
Normal stiffness [GPa/m]	Shear stiffness [GPa/m]	Residual hydraulic aperture [mm]	Aperture at zero normal stress [mm]
3	1	1.0	1.0

The cubic law, on the other hand, which explains the flow rate of a Newtonian fluid within two parallel plates with an aperture of a is written as

$$q = \frac{1}{12\mu_g} a^3 \frac{\Delta p}{L} \tag{2}$$

From Eq. (1), it can be observed that the fluid flow will not occur when the pressure gradient ($\Delta p/L$) is either zero or equals to the ratio of $2\tau_0/r$ meaning that the Bingham fluid flow takes place only when the pressure gradient exceeds the threshold value of $2\tau_0/r$.

Since cement grout is injected at the center of circular specimen, only one-fourth of the joint specimen is to be modelled and results of penetration are shown in the following figures. It is the pressure difference between injected cement grout and initial pore fluid inside the joint that drives the cement grout flow. In this study, an initial dry condition for the joint and a pressure gradient was applied to induce a flow in numerical simulation. At every moment of analysis, the radius of the circle, within which the fluid saturation ratio of infilled joints is turned into one from zero, can be regarded as the grout penetration length. The Material properties required in the numerical simulations are the same as the previous study (Kim *et al.* 2018) and was summarized in Table 2. It should be noted that the material properties in the table are mainly from intact rock and they can be different from those of acryl plates in the experiment. However, their influence should be negligible since the mechanical deformation of discrete joint is hardly induced due to the low injection pressure condition in the experiments.

3.1 Comparison of penetration length between experimental observation and numerical estimation

3.1.1 The effect of W/C ratio

Fig. 7 compares the penetration lengths of a reference case at two different *W/C* ratios. In the reference case, an injection rate of 200 ml/min and a joint aperture of 1 mm were used. The average value of penetration lengths obtained from four different experimental measurements was calculated and compared with the numerical estimation. One typical example of penetration behavior in the

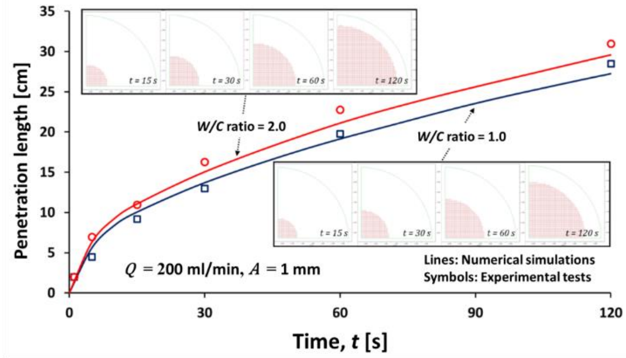

Fig. 7 The penetration lengths obtained from experimental observations and numerical estimations at different *W/C* ratios (Note that the 1/4th of the numerical simulation results were shown on the figure and one typical example of experimental observation was shown in Fig. 5)

experiments was shown in Fig. 4 and the one in the numerical simulation, at which only the one-fourth of the circular joint model was considered, was shown together in this figure. Although a variation in the experimental measurements was observed at each elapsed times of 15, 30, 60 and 120 seconds, the overall penetration lengths, in the reference cases, under both *W/C* ratios of 1.0 and 2.0 were well comparable to the numerical estimations.

3.1.2 The effect of injection flow rate and joint aperture

Figs. 8 and 9 show the comparison of penetration length under different injection rates and joint apertures, respectively. The results of experimental observations and numerical estimations exhibit a reasonable agreement particularly in the lower injection rate and smaller joint aperture condition. However, the difference of penetration lengths between two approaches became more distinct as the injection rate and joint aperture were increased. The overestimation in the experimental observation is caused by material characteristics (; bleeding) and the flowing behavior of cement grout in larger aperture and higher *W/C* ratio (Lee *et al.* 2017 and 2019). It is noted that the present numerical approach, which is based on a simple laminar flow and single phase fluid, can rarely be used in these specific conditions. It may be beyond the scope of the current work but, this difference can be reduced by applying a more complex multi-phases and multi-components fluid flow model to reproduce a bleeding in cement grout.

Air bubbles contained in a cement grout, which is also known to influence the grout flow and performance (Warner, 2004), may contribute this difference in a certain extent but, their effect should be more influential in deteriorating water proof performance rather in penetration length.

3.2 The effect of time dependent viscosity of cement grout

In numerical simulations, the effect of time-dependency in viscosity of cement grout can be investigated with ease

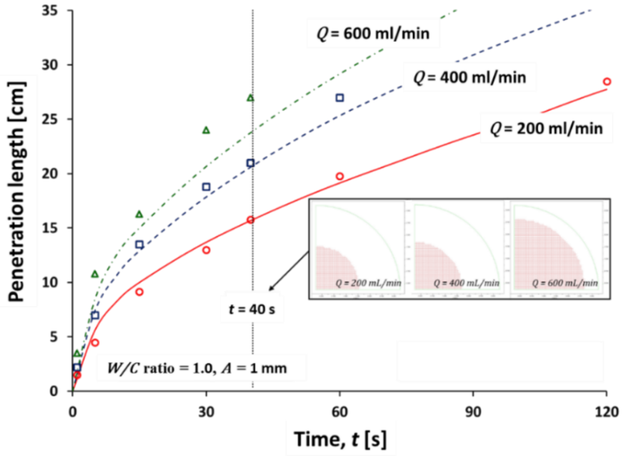

Fig. 8 The penetration lengths obtained from experimental observations (symbols) and numerical estimations (lines) under different injection rate conditions (Note that the 1/4th of the numerical simulation results were shown on the figure and one typical example of experimental observation was shown in Fig. 3)

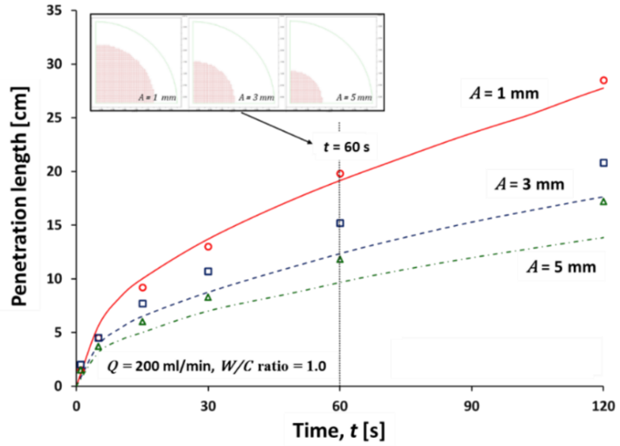

Fig. 9 The penetration lengths obtained from experimental observations (symbols) and numerical estimations (lines) under different joint aperture conditions. (Note that the 1/4th of the numerical simulation results were shown on the figure and one typical example of experimental observation was shown in Fig. 4)

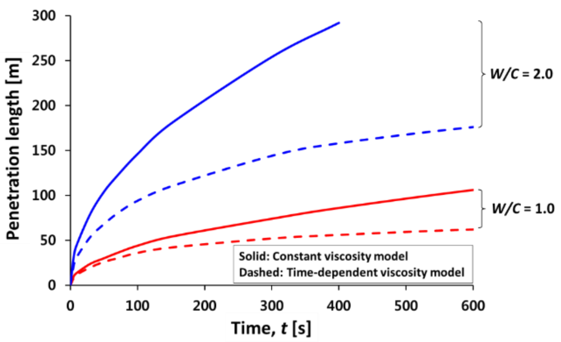

Fig. 10 The penetration lengths with and without time-dependent evolution of the cement grout viscosity during the period of injection

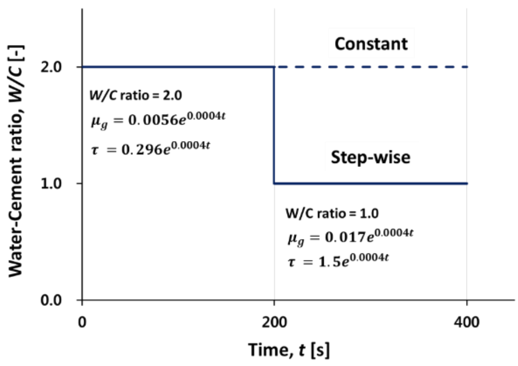

(a) Step-wise W/C ratio change

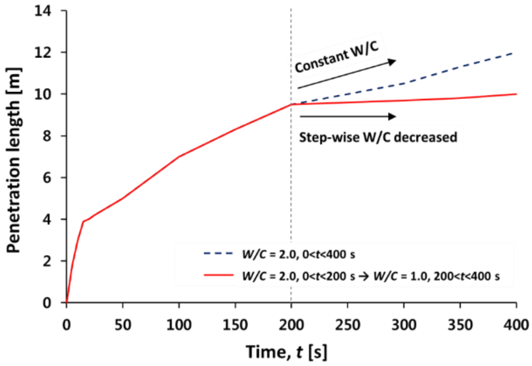

(b) Penetration length

Fig. 11 The effect of step-wise W/C ratio change on grout penetration length

from a comparison between the values of penetration lengths obtained with and without this time-dependency. The time-dependency of grout viscosity was defined, in numerical model, using a function of time elapse after injection. In the case of without time-dependency, the viscosity was kept constant during the time period of injection. Fig. 10 illustrates the results of simulations with and without time-dependency effects for two different W/C ratios in which a large reduction in penetration lengths could be distinctly observed when this effect was considered. In other words, the grout penetration length can be highly overestimated when the time-dependency in cement grout viscosity is ignored. Therefore, the time dependent viscosity of cement grout should be recognized as one of the significant factors involved in estimating grout performance and designing grouting work.

3.3 The effect of W/C ratio change

W/C ratio can be varied to control a grout performances, since higher W/C may produce longer penetration length due to its lower viscosity. Lower W/C ratio, meanwhile result in less penetration length but, should have more efficient waterproof performance thanks to relatively denser concentration of cement (Lee 2017). In this study, a simple case of step-wise change of W/C ratio in the course of injection was examined by numerical simulation. W/C ratio was decreased in a step-wise manners and compared with the results of consistent injection to demonstrate how significantly the penetration performance can be different.

Fig. 11 presents two distinct scenarios of *W/C* conditions and their properties; one is continuous injection with *W/C* ratio of 2 throughout a whole injection period of 400 seconds, and the other is that *W/C* ratio is reduced to 1 in the course of injection at the elapsed time of 200 seconds. It is clearly seen that the penetration length is reduced in the step-wise decreasing manner of *W/C* ratio due to its higher viscosity at longer elapsed time. However, it should be noted that the grout injection of a tunnel with lower *W/C* ratio produces higher waterproof performance due to its denser cement concentration. Therefore, site-specific scenarios for the variation of *W/C* ratio can be effectively determined, using this kind of numerical approach, to have an optimum penetration length and cement concentration around a tunnel.

4. Conclusions

In this study, we investigated a cement grout penetration behavior in discrete joints both experimentally and numerically. The grout penetration lengths, in the experiments, were measured under different conditions of injection rates and joint apertures and then compared to the estimations by numerical simulation. In the numerical estimations, the well-known Bingham fluid model was used to simulate viscous cement grout flow in discrete joints.

Although both experimental measurements and numerical estimations of penetration length were comparable in the specific conditions with smaller joint aperture and lower water-cement ratio, discrepancy could be observed in the comparison. The difference between experimental and numerical results in penetration length tends to be resulting from material separation (; bleeding) of cement grout mix and was much more dominant in those experimental conditions with larger joint aperture, higher water-cement ratio and larger flow rate. The surface friction of joint wall and air bubbles entrained in a cement grout may contribute this difference. Although this study was performed with considering grout flow in a smooth fracture, the grout penetration can be further affected by the characteristics of fracture such as roughness and saturation conditions and even its connections in the natural fractures. Therefore, it should be noted that the estimation of penetration length by numerical simulation can be only applicable in limited conditions and a multi-phase and multi-components fluid flow model may be required, in a numerical approach, for more practical and precise designing of cement grout.

In the experiments, we also measured the viscosity variation of a cement grout as a function of elapsed time after injection to construct a time-dependent model for a cement grout viscosity. The constructed time-dependent model was implemented in the numerical simulations to examine the effect of the time-dependent viscosity on a grout penetration length. Our numerical simulations showed that the grout penetration length can be considerably overestimated when the time-dependent evolution of grout viscosity is not considered. It was also demonstrated, by the numerical simulation, a step-wise reduction of *W/C* ratio at a later time of injection can be more effective in grout penetration region and waterproof performance of the grouted region in the vicinity of a tunnel.

Acknowledging the simulation results in this study were obtained from the simplified cases, the numerical approach of a discrete joint model could be practically used in optimizing overall grout design in jointed rock mass by further improving a fluid flow model and being extended to a coupled mechanical-hydraulic analysis in discrete joint network model.

Acknowledgments

This research was supported by the Basic Research Project of the Korea Institute of Geoscience and Mineral Resources (KIGAM) and by the Basic Science Research Program through the National Research Foundation of Korea (KRF) that is funded from the Ministry of Science and ICT of Korea (2017R1A2B4002280).

References

Azimian, A. and Ajalloeian, R. (2015), "Permeability and groutability appraisal of the Nargesi dam site in Iran based on the secondary permeability index, joint hydraulic aperture and Lugeon tests", *Bull. Eng. Geol. Environ.*, **74**(3), 845-859. https://doi.org/10.1007/s10064-014-0675-8.

Funehag, J. and Thörn, J. (2018), "Radial penetration of cementitious grout–Laboratory verification of grout spread in a fracture model", *Tunn. Undergr. Sp. Technol.*, **72**, 228-232. https://doi.org/10.1016/j.tust.2017.11.020.

Ghafar, A.N., Sadrizadeh, S. and Magakis, K. (2017), "Varying aperture long slot (VALS), a method for studying grout penetrability into fractured hard rock", *Geotech. Test. J.*, **40**(5), 871-882. https://doi.org/10.1520/GTJ20160179.

Gustafson, G. and Stille, H. (1996), "Prediction of groutability from grout properties and hydrogeological data", *Tunn. Undergr. Sp. Technol.*, **11**(3), 325-332. https://doi.org/10.1016/0886-7798(96)00027-2.

Gustafson, G. and Stille, H. (2005), "Stop criteria for cement grouting", *Felsbau*, **23**, 62-68.

Gustafson, G., Claesson, J. and Fransson A. (2013), "Steering parameters for rock grouting", *J. Appl. Math.*, 1-9. http://dx.doi.org/10.1155/2013/269594.

Hakansson, U., Hassler, L. and Stille, H. (1992), "Rheological properties of microfine cement grouts", *Tunn. Undergr. Sp. Technol.*, **7**(4), 453-458. https://doi.org/10.1016/0886-7798(92)90076-T.

Houlsby, A.C. (1990), *Construction and Design of Cement Grouting: A Guide to Grouting in Rock Foundations*, John Wiley & Sons Inc., Hoboken, New Jersey, U.S.A.

Itasca (2014), *UDEC User's Manual Ver.6.0*, Itasca Consulting Group Inc., Minneapolis, Minnesota, U.S.A.

Jamsawang, P., Poorahong, H., Yoobanpot, N. and Jongpradist, P. (2017), "Improvement of soft clay with cement and bagasse ash waste", *Construct. Build. Mater.*, **154**, 61-71. https://doi.org/10.1016/j.conbuildmat.2017.07.188

Jones, B.R., Louis Van Rooy, J. and Mouton, D.J. (2018), "Verifying the ground treatment as proposed by the Secondary Permeability Index during dam foundation grouting", *Bull. Eng. Geol. Environ.*, **78**(3), 1305-1326. https://doi.org/10.1007/s10064-017-1219-9

Kim, H.M., Lee, J.W., Yazdani, M., Tohidi, E., Nejati, H.R. and Park, E.S. (2018), "Coupled viscous fluid flow and joint deformation analysis for grout injection in a rock joint", *Rock Mech. Rock Eng.*, **51**(2), 627-638. https://doi.org/10.1007/s00603-017-1339-3.

Kobayashi, S. and Stille, H. (2007), "Design for rock grouting based on analysis of grout penetration", Verification using Äspö HRL data and parameter analysis, No. SKB R-07-13, Swedish Nuclear Fuel and Waste Management Company, Stockholm, Sweden.

Lee, H.B., Oh, T.M., Park, E.S., Lee, J.W. and Kim, H.M. (2017), "Factors affecting waterproof efficiency of grouting in single rock fracture", *Geomech. Eng.*, **12**(5), 771-783. https://doi.org/10.12989/gae.2017.12.5.771.

Lee, J.W. (2017), "Performance analysis on the design parameters of viscous fluid penetration in rock joint", M.Sc. Thesis, Sejong University, Seoul, Korea.

Lee, J.W., Oh, T.M., Kim, H. and Kim, M.K. (2019), "Coupling material characteristics with water-cement ratio for elastic wave based monitoring of underground structure", *Tunn. Undergr. Sp. Technol.*, **84**, 129-141. https://doi.org/10.1016/j.tust.2018.11.014.

Li, S.C., Sha, F., Liu, R.T., Zhang, Q.S. and Li, Z.F. (2017), "Investigation on fundamental properties of microfine cement and cement-slag grouts", *Construct. Build. Mater.*, **153**, 965-974. https://doi.org/10.1016/j.conbuildmat.2017.05.188.

Minto, J.M., Mac Lachlan, E., Mountassir, G.E. and Lunn, R.J. (2016), "Rock fracture grouting with microbially induced carbonate precipitation", *Water Resour. Res.*, **52**(11), 8827-8844. https://doi.org/10.1002/2016WR018884.

Mohammed, M.H., Pusch, R. and Knutsson, S. (2015), "Study of cement-grout penetration into fractures under static and oscillatory conditions", *Tunn. Undergr. Sp. Technol.*, **45**, 10-19. https://doi.org/10.1016/j.tust.2014.08.003.

National Research Council (NRC). (1996), *Rock Fractures and Fluid Flow: Contemporary Understanding and Applications*, National Academies Press, Washington, D.C., U.S.A.

Rahman, M., Wiklun, J., Kotze, R. and Hakansson, U. (2017), "Yield stress of cement grouts", *Tunn. Undergr. Sp. Technol.*, **61**, 50-60. https://doi.org/10.1016/j.tust.2016.09.009.

Saedi, O., Stille, H. and Torabi, S.R. (2013), "Numerical and analytical analyses of the effects of different joint and grout properties on the rock mass groutability", *Tunn. Undergr. Sp. Technol.*, **38**, 11-25. https://doi.org/10.1016/j.tust.2013.05.005.

Sohrabi-Bidar, A., Rastergar-Nina, A. and Zolfaghari, A. (2016), "Estimation of the grout take using empirical relationship (case study: Bakhtiari dam site)", *Bull. Eng. Geol. Environ.*, **75**(2), 425-438. https://doi.org/10.1007/s10064-015-0754-5.

Struble, L. and Sun, G.K. (1995), "Viscosity of Portland cement paste as a function of concentration", *Adv. Cem. Based Mater.*, **2**(2), 62-69. https://doi.org/10.1016/1065-7355(95)90026-8.

Sui, W., Liu, J., Hu, W., Qi, J.F. and Zhan, K. (2015) "Experimental investigation on sealing efficiency of chemical grouting in rock fracture with flowing water", *Tunn. Undergr. Sp. Technol.*, **50**, 239-249. https://doi.org/10.1016/j.tust.2015.07.012.

Tani, M.E. and Stille, H. (2017), "Grout spread and injection period of silica solution and cement mix in rock fractures", *Rock Mech. Rock Eng.*, **50**(9), 2365-2380. https://doi.org/10.1007/s00603-017-1237-8.

Warner, J. (2004), *Practical Handbook of Grouting: Soil, Rock and Structures,* John Wiley & Sons, Inc., Hoboken, New Jersey, U.S.A.

Wilkinson, W.L. (1960), *Non-Newtonian Fluid: Fluid Mechanism Mixing and Heat Transfer*, Pergamon Press, London, U.K,.

Xiao, F., Zhao, Z. and Chen, H. (2017), "A simplified model for predicting grout flow in fracture channels", *Tunn. Undergr. Sp. Technol.*, **70**, 11-18. https://doi.org/10.1016/j.tust.2017.06.024.

Zheng, G., Zhang, X., Diao, Y. and Lei, H. (2016), "Experimental study on the performance of compensation grouting in structured soil", *Geomech. Eng.*, **10**(3), 335-355. https://doi.org/10.12989/gae.2016.10.3.335.

JS